

# PROCEEDINGS OF SPIE

[SPIDigitalLibrary.org/conference-proceedings-of-spie](https://spiedigitallibrary.org/conference-proceedings-of-spie)

## Calibrating the sag due to gravity of horizontal interferometer reference flats

Burke, Jan, Griesmann, Ulf

Jan Burke, Ulf Griesmann, "Calibrating the sag due to gravity of horizontal interferometer reference flats," Proc. SPIE 8493, Interferometry XVI: Techniques and Analysis, 84930F (13 September 2012); doi: 10.1117/12.929968

**SPIE.**

Event: SPIE Optical Engineering + Applications, 2012, San Diego, California, United States

# Calibrating the sag due to gravity of horizontal interferometer reference flat

Jan Burke<sup>a,b</sup> and Ulf Griesmann<sup>c</sup>

<sup>a</sup>Australian Centre for Precision Optics, Commonwealth Science and Industrial Research Organization, Bradfield Road, Lindfield NSW 2070, Australia;

<sup>b</sup>Bremer Institut für Angewandte Strahltechnik (BIAS), Klagenfurter Str. 2, 28359 Bremen, Germany;

<sup>c</sup>National Institute of Standards and Technology (NIST), Physical Measurement Laboratory, Gaithersburg, MD 20899-8223, USA

## ABSTRACT

We describe a method for measuring the deflection due to gravity (sag) of horizontally mounted reference flat of phase shifting interferometers. The planarity of a test flat can be measured sag-free while supporting it iso-statically on a suitable visco-elastic polymer foam. A sag map is obtained when the sag-free flatness error is subtracted from the flatness error of the same flat held at its edge.

**Keywords:** Optical interferometry, Reference flat calibration, Sag

## 1. INTRODUCTION

Three-flat tests are a well-understood procedure for determining the planarity, or flatness error, of interferometer reference flats<sup>1-10</sup>. A flat test requires the pairwise comparison of flat with an interferometer, as is schematically indicated in Fig. 1. In most cases a flat test will be performed using a Fizeau interferometer, because this type of interferometer can achieve very low measurement uncertainty. In a Fizeau interferometer all optics (not shown in Fig. 1) are shared by both test and reference arms of the interferometer, and in this “common path” configuration phase errors in the imaging system are identical in reference and test beams and cancel out. For three circular, nominally identical flats *A*, *B*, and *C*, a three flat test consists of at least the four measurements  $M_1$ ,  $M_2$ ,  $M_3$ , and  $M_4$  of Fig. 1. The measurements in Fig. 1 can be translated into an equation involving the planarities of the flats

$$\begin{pmatrix} M_1(x, y) \\ M_2(x, y) \\ M_3(x, y) \\ M_4(x, y) \end{pmatrix} = \begin{pmatrix} 1 & 0 & 1 & 0 & 0 \\ 0 & 0 & 1 & 0 & 1 \\ 1 & 0 & 0 & 1 & 0 \\ 0 & 1 & 0 & 1 & 0 \end{pmatrix} \begin{pmatrix} A(x, y) \\ B(x, y) \\ B(-x, y) \\ C(-x, y) \\ A^R(r) \end{pmatrix}. \quad (1)$$

In Eq. 1  $A(x, y)$ ,  $B(x, y)$ , and  $C(x, y)$  stand for the flatness errors of flat *A*, *B*, and *C* respectively.  $M_1$  is a measurement of the test flat *A* against reference flat *B* (reference flat *B* are shown above the test flat *A* in Fig. 1). The result is the combined flatness error of flat *A* and *B*. Likewise,  $M_3$  is a measurement of test flat *A* against reference flat *C*, and in  $M_4$ , test flat *B* is measured against reference flat *C*. In this measurement sequence (BA, CA, CB), as in all three-flat test procedures, at least one of the flats must be used as both test- and reference flat. In addition to these measurements a fourth measurement is required in which one of the flats is rotated. This additional measurement is  $M_2$  in Fig. 1 and Eq. 1.  $A^R(r)$  denotes the rotation average of the planarity of flat *A*. The measurement of a flat here *B*, against the rotation average of another can

Author contact emails: burke@bias.de, ulf.griesmann@nist.gov

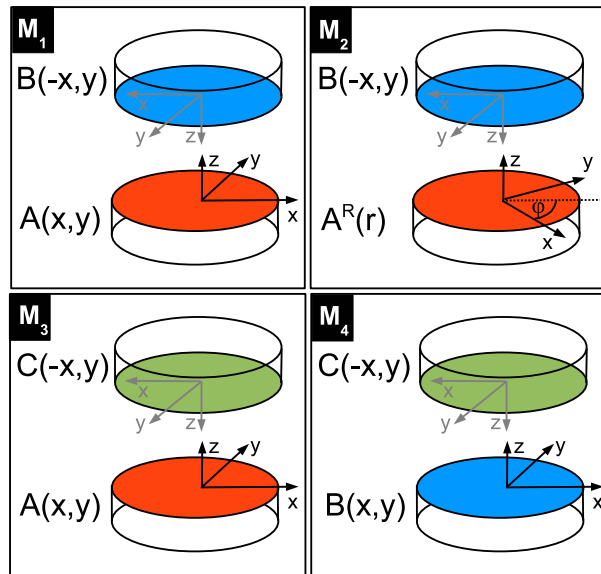


Figure 1. One possible set of measurements comprising a three-fla test.

be accomplished using either N-position averaging<sup>4,6,10</sup> or rotational shear measurements.<sup>2,5</sup> Eq. 1 can be solved for the flatness errors of the three flats<sup>6,9</sup> and one possible solution is:

$$\begin{pmatrix} A(x, y) \\ B(x, y) \\ C(x, y) \end{pmatrix} = \frac{1}{2} \begin{pmatrix} 1 & 1 & -1 & 2 & -2 & 0 \\ 1 & -1 & 1 & 0 & -2 & 0 \\ -1 & 1 & 1 & 2 & -2 & -2 \end{pmatrix} \begin{pmatrix} M_1^e(x, y) \\ M_3^e(x, y) \\ M_4^e(x, y) \\ M_1^o(x, y) \\ M_2^o(x, y) \\ M_3^o(x, y) \end{pmatrix}, \quad (2)$$

where  $M_k^e(x, y) = M_k^e(-x, y)$  are the even components of  $M_k$  under reflection at the y-axis,  $M_k^o(x, y) = -M_k^o(-x, y)$  the odd components, and  $M_k^e(x, y) + M_k^o(x, y) = M_k(x, y)$ .

When interferometer flats are mounted horizontally and supported at their edges, as shown in Fig. 1, they are unavoidably deflected by the force of gravity. This deflection or sag, is *not* included in the three-fla test described by Eq. 1 and its solution Eq. 2. In the three-fla test shown in Fig. 1, the sags of flat A and C can be ignored as long as they are nominally identical, as both of them are always tested in the same orientation; however, due to the inevitable flipping of at least one fla (fla B in Fig. 1), the sag must be well characterized, and the sag measured in the “test” position ( $M_4$ ) must be assumed to be the same, but with opposite sign, as that in the “reference” position ( $M_1, M_2$ ). An additional, separate sag measurement is necessary because the sag can be determined only partially as part of the the three-fla calibration.<sup>11</sup>

Already in 1966, G. Dew remarked: “In view of the frequent use that is made of three point edge supports for interferometer flats it is surprising that so few attempts have been made to measure the sag experimentally”.<sup>12</sup> This observation remains valid today. Even though it is not uncommon that horizontally mounted fla surfaces must be characterized, the problem of finding a reliable experimental procedure for calibrating the sag of reference flats due to their weight has proven to be refractory and few solutions have been suggested in the literature, especially ones that are suitable for production environments.

A well known solution for the calibration of a horizontally mounted interferometer reference fla is the use of a liquid mirror as an absolute flatness standard.<sup>13-15</sup> Mercury mirrors have been used successfully as flatness standards,<sup>13</sup> but more recent realizations of liquid flats have relied on silicon oil surfaces to avoid the health risk caused by mercury. Despite their conceptual simplicity, liquid flats have several disadvantages. It is obvious, that they are not strictly flats but are spherical surfaces with the radius of the earth. This becomes unacceptable when precision surfaces must be tested with nm level uncertainty. Silicone oil reference surfaces can also be affected by thermal gradients in the oil and electrical forces due to

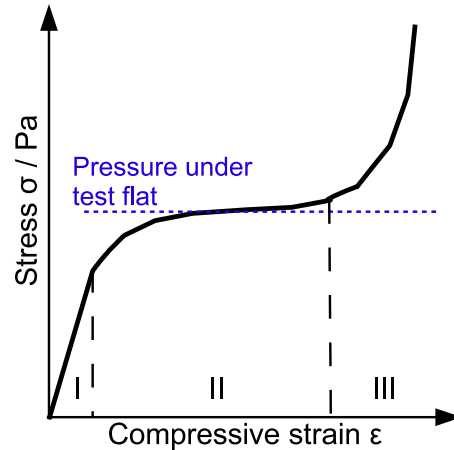


Figure 2. Static stress as a function of uniaxial compressive strain for a polymer foam material.

electric charges on the non-conductive oil. Overall, the uncertainties that have been reported for silicon oil reference flat are at least about 3 nm,<sup>14,15</sup> which is too high for demanding applications.

A more practical solution was advanced by Vannoni and Molesini<sup>11</sup> who eliminated the gravitational sag of a test fla with 150 mm diameter by supporting it on a membrane covering a pressurized air cell. The flatnes of the membrane supported fla was subtracted from the flatnes of the same fla when it was held at three points at its edge to obtain the gravitational sag. The experimental results agreed with numerical finite-elemen calculations of the sag.

In this paper we return to a similar, earlier idea by Fairman *et al.*<sup>16</sup> and Oreb *et al.*<sup>17</sup> who describe the calibration of the sag due to gravity for the 350 mm diameter reference flat of the Large Aperture Digital Interferometer (LADI) at CSIRO, Australia. A polymer foam sheet of about 3 mm thickness was used to support the test fla iso-statically to eliminate the sag due to gravity. The same test fla was then measured while held at its edge. The difference of the two measurements is the sag due to gravity. The procedure gave satisfactory results but it was never followed up by a careful analysis of the method.

The foundation for the work presented in the following sections is contained in Fig. 2, which shows the *static* stress  $\sigma$  in a polymer foam material resulting from an uniaxial compressive strain  $\varepsilon$ . Compressive strain is define by the equation:

$$\varepsilon = \frac{\Delta\tau}{\tau}, \quad (3)$$

where  $\tau$  is the thickness of the material before compression, and  $\Delta\tau$  the amount of compression. The *static* stress-strain curve of all polymer foams has the characteristic shape shown in Fig. 2.<sup>18,19</sup> It can be understood qualitatively by considering the structure of a typical polymer foam material. A scanning electron microscopy (SEM) image of the surface of an open-cell polyurethane foam sheet is shown in Fig. 3. At small strains, the response of the foam is linear (region I). Once the strain is increased beyond a certain threshold, the cells of the foam (see Fig. 3) begin to collapse and the stress increases only slowly as the strain is increased and more cells collapse (region II). Finally, when all foam cells have collapsed the material is compacted and the stress rises rapidly as the material properties approach those of the bulk material (region III). When a glass fla with diameter  $D$  is placed on a sheet of foam, the pressure  $p$  under the glass plate is

$$p = \rho \cdot t \cdot g \quad (4)$$

where  $\rho$  is the density of the glass,  $t$  the thickness of the plate, and  $g$  the acceleration due to gravity ( $g = 9.80665 \text{ m}\cdot\text{s}^{-2}$  at sea level). For example, for a 70 mm thick silica glass fla with a density of  $2.21 \text{ g}\cdot\text{cm}^{-3}$ , the pressure under the fla is approximately 1500 Pa. When this pressure coincides with the plateau in the stress-strain curve of the foam sheet, the reactive pressure by the foam is nearly constant for a wide range of strains and the support of the fla is quasi-iso-static.

The striking capacity of visco-elastic foam mats to iso-statically support a fla on an uneven surface, or table, is illustrated by the experiment that is shown in Fig. 4. Four steel shims with  $50 \mu\text{m}$  (right),  $100 \mu\text{m}$  (front),  $200 \mu\text{m}$  (left), and

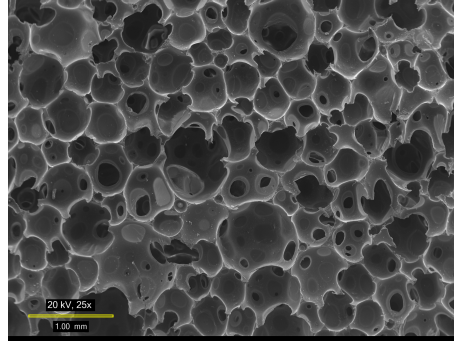


Figure 3. Scanning electron micrograph of the cellular foam structure at the top surface of one of the open-cell polyurethane foams used in this study.

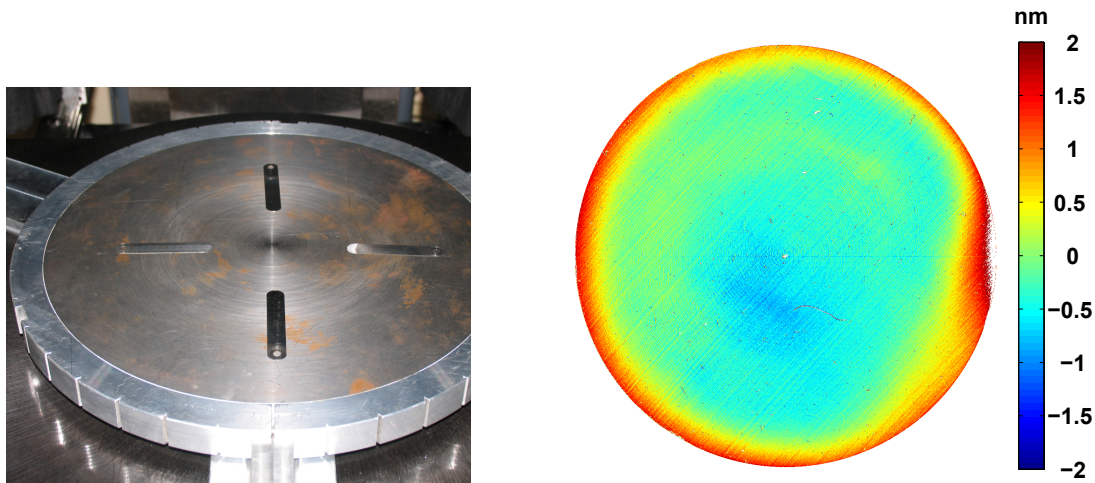


Figure 4. Shims with thicknesses of  $50\ \mu\text{m}$  (right),  $100\ \mu\text{m}$  (front),  $200\ \mu\text{m}$  (left), and  $300\ \mu\text{m}$  (back), placed under a polyurethane foam mat (left image). Difference of two measurements of reference flange A against test flange C with and without the shims (right image).

$300\ \mu\text{m}$  (back) thickness were placed on the rotary table of the LADI interferometer (left image in Fig 4). Table and shims were covered with a 3 mm thick, visco-elastic polyurethane foam mat, and test flange C was lowered onto the foam sheet<sup>20</sup> and the flange was measured against reference flange A. This was followed by a measurement without the shims under the foam sheet. The difference of the two measurements is shown on the right side of Fig. 4. No features in the difference map can be correlated with the location of the shims that were placed under the foam mat.

In section 2 we summarize the mechanical properties of the foam materials that were used to support flats. Section 3 describes how the polymer foams were applied to measuring the sag due to gravity of the reference flat of the LADI with 350 mm diameter.

## 2. POLYMER FOAMS

A number of visco-elastic foams made from silicone, polyurethane, and neoprene were investigated. In addition, we explored several visco-elastic silicone gels and other gel materials for this application. The static stress-strain curves of these materials were measured at an ambient temperature of about  $24\ ^\circ\text{C}$  using the testing instrument shown in Fig. 5. Foam specimens were prepared for compression testing by cutting 25 mm diameter discs from foam sheets using a hollow punch which matched the 25 mm diameter platens of the testing machine (see inset in Fig 5). The foam sheets were either 3 mm or 6 mm thick. In some cases the thinnest commercially available sheet was 10 mm thick. The silicone gels were purchased either as sheets, or in liquid form and cast in a mold to create approximately 6 mm thick gel sheets. In the compression tester, the foam and gel sheets were compressed by a specific amount and, after relaxation of the material, the compression

force was measured. Most of the visco-elastic foams will continue to relax even for several hours after compression, but after about 20 min the changes in the compressive force became very small. In most cases the force measurements were made 20 min to 30 min after changing the compressive strain. Fig. 6 shows static stress–strain curves that were obtained for several types of materials. One of the curves (SS6080) in the diagram for a soft silicone gel. This silicone gel, like other silicon gels, shows an almost purely elastic response to compression with a steep slope in the stress–strain diagram. The silicone gels are even less compressible than the curve in the stress–strain diagram Fig. 6 indicates. When a compressive force is applied to the platens of the compression tester, the silicon gels were pushed out in radial direction from between the platens. The steep slopes of the stress–strain diagrams for silicone gels at the pressures that are found under typical optical reference flat makes these materials unsuitable as an iso-static support material. The two silicone foams, Saint-Gobain AGP200<sup>†</sup> and Rogers BF2000<sup>†</sup>, in Fig. 6 have quite different stress–strain diagrams. BF2000 has an almost elastic behavior that is very similar to a gel. This is related to the structure of the foam. BF2000 is a foam with nearly closed cells, and top and bottom sides of the foam are sealed. AGP200 is an open cell foam with clear plateau behavior. BF2000 and AGP200 were the two softest silicone foams that seemed to be commercially available. These foams are typically produced as gasket materials and most silicone foams are too firm to be useful as iso-static reference flat supports. The same holds for the rubber and neoprene foams that were investigated. Without exception, they were not sufficiently soft to reach the plateau in Fig 2 for the pressures under our optical flats. Also shown in Fig. 6 are stress–strain curves for three different viscoelastic 3M CONFOR<sup>†</sup> polyurethane foams. It is evident that the polyurethane foams have mechanical properties that make them better suited for our intended application. The stresses at which the plateaus in the stress–strain diagram occur cover the range of pressures under typical interferometer flat with several cm thickness. In addition to the foams shown in Fig. 6, a number of soft, visco-elastic polyurethane foams sheets with thicknesses of 3 mm and 6 mm from another supplier, Bergad<sup>†</sup>, was investigated. The stress–strain diagrams for these foams are shown in Fig. 7.

The uncertainty of the static stress measurements is determined by the specimen preparation and the measurement of the compressive force after complete relaxation of the foam following compression. The strain  $\sigma$  is proportional to the compression force  $F$ :

$$\sigma = \frac{4F}{\pi D^2}, \quad (5)$$

where  $D$  is the diameter of the cylindrical foam specimen. Using a hollow punch, the foam specimens could be prepared with a diameter uncertainty  $\delta D$  of about 0.5 mm. The corresponding uncertainty for the stress is:

$$\delta\sigma = 2\sigma \frac{\delta D}{D}. \quad (6)$$

For a stress of 1500 Pa, which corresponds to the pressure under a 70 mm thick silica glass flat the stress uncertainty due to the specimen preparation is about 60 Pa. The uncertainty due to the compression force measurement is negligible. Another contributor to the measurement uncertainty is the uncertainty in the strain, which mostly depends on the measurement of the foam specimen thickness. For the thickness measurement a foam sample was loaded on the bottom platen in the testing machine (see Fig. 5), and the top platen was lowered slowly until the platen touched the foam and the compression force began to rise. In this way the specimen thickness could be determined with an uncertainty of 2  $\mu\text{m}$ . The resulting strain uncertainty is negligible. The uncertainty of the compression force measurement in the fully relaxed state is the most difficult to quantify. Force measurements were made between 20 min to 30 min after compression, because at that time the force had either stabilized or was changing only very slowly for all foams. Due to the limited time available it was not possible to wait for complete relaxation after each compression step. We estimate the resulting uncertainty for the stress to be smaller than the uncertainty due to the specimen preparation.

### 3. SAG MEASUREMENT

The Large Aperture Digital Interferometer (LADI) that is used for low-uncertainty measurements at CSIRO's Australian Centre for Precision Optics has a vertical axis and the glass flat used are therefore subject to gravitational deformation.<sup>16,17</sup> There is ample theory on the expected bending of a circular plate supported at the edge,<sup>21–23</sup> and the challenge is to build a support that will work the same way for both orientations of the reflective surface. CSIRO has constructed symmetrical ring supports from high-stiffness aluminum that hold the calibration flat via 18 elastic pads; the aluminum rings themselves are then mounted in the interferometer or the calibration assembly with a three-point kinematic support. For the dimensions and mechanical parameters of the flat used, the expected sag is 27 nm.<sup>23</sup> The sag of the designated reference flat was not

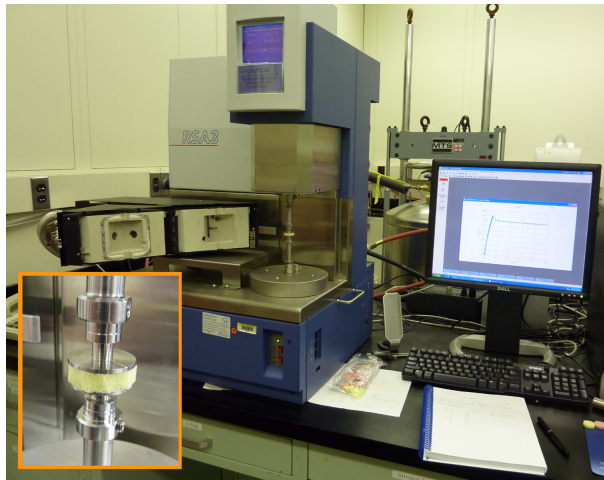


Figure 5. Testing machine for stress–strain curve measurements of polymer foam materials.

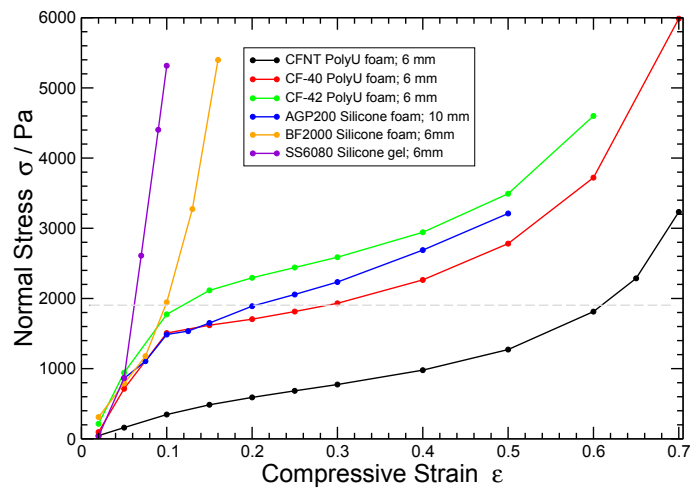


Figure 6. Stress–strain diagrams for several materials.

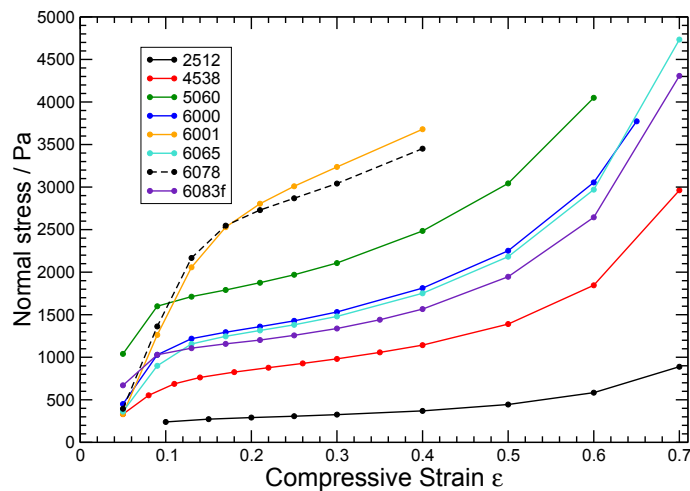


Figure 7. Stress–strain diagrams for viscoelastic polyurethane foams.

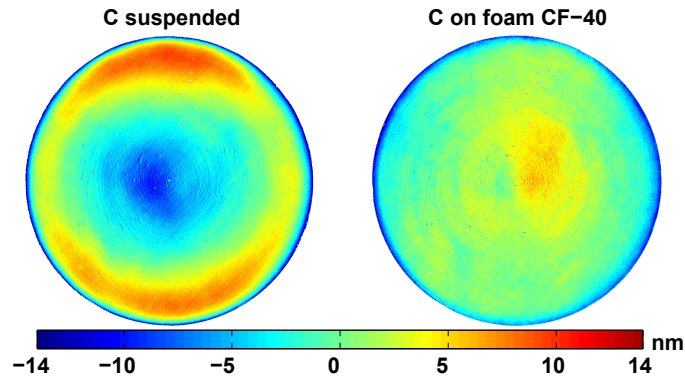


Figure 8. LADI reference flat A against test flat C suspended and on foam CF-40.

measured, as it is always used with the reflective face down; however the two other calibration flats were both tested for amount and reproducibility of the sag. First the respective flat was suspended in the 3-point mount and left to settle over night. Then 10-20 measurements of the OPD against the reference flat were taken and averaged. After the results were verified to be consistent (reproducibility rms < 0.5 nm), the flat was taken out of the 3-point mount, set on a foam pad and left to settle over night again. A thin sheet of black silk was placed between the glass and the foam to eliminate the adhesion of the foam to the glass and make it possible to adjust the position of the flat once it has been set down on the foam mat. Fig. 8 shows measurements of LADI reference flat A against test flat C first suspended at the edge and then on a foam mat (Bergad 6083f). Flat A of the LADI interferometer is figured to compensate for the sag. Its reference surface is almost plane when the flat is held by the edge. When the difference of the two maps is calculated, the flatness error of flat A and the system error cancel out. The result is the sag due to gravity for flat C, which is shown in Fig. 9.

It is instructive to compare the measured sag due to gravity with the deflection calculated using the formula by Selke.<sup>23</sup> This is done in Fig. 10. Shown are diameters in x- and y-directions of sag measurements for flat C that were made with two different foam mats. For one of the foams (CF-40) the agreement for both diameters is very good and the sag curves also agree qualitatively with the theoretical sag curve. Large deviations from the theoretical sag are observed near the edge of the flat. The flat support system appears to cause a much more complex bending behavior than is expected from the idealized boundary conditions of the theoretical model. For the second foam (6083f) the two orthogonal sag curves differ and the sag map has an astigmatism that is absent in the measurement with the CF-40 foam. This discrepancy can be traced back to the procedure for lowering the flat onto the foam mat. The most reproducible results with minimal astigmatism were achieved

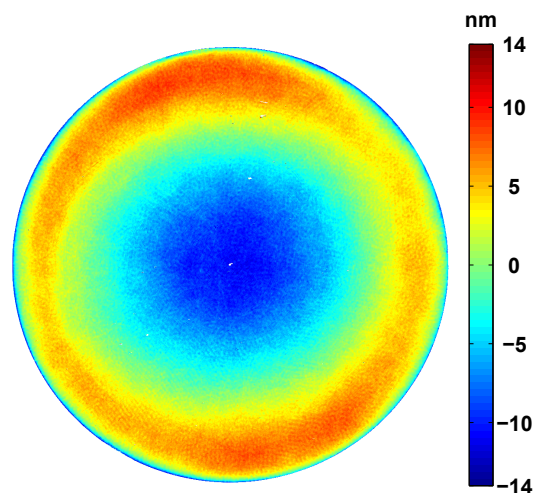


Figure 9. Sag due to gravity for LADI flat C.

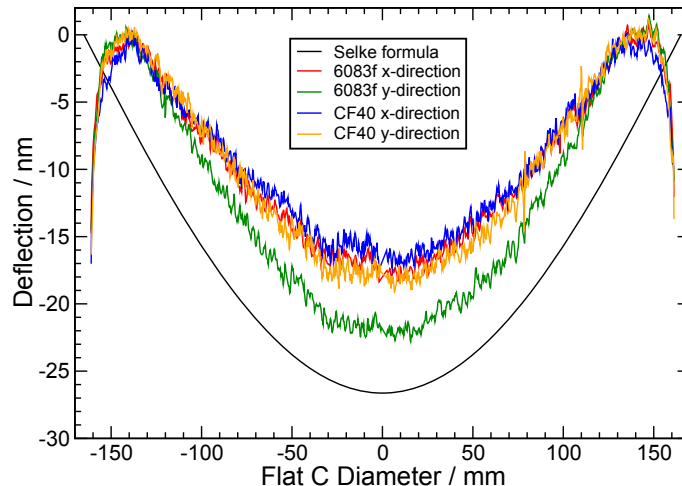


Figure 10. Theoretical deflection due to gravity of a plate that is suspended at its edge<sup>23</sup> (black), and experimental deflection for diameters in x- and y-direction measured with two different polyurethane foam mats.

when the flat was lowered onto the foam slowly and in such a way that the entire bottom surface of the flat makes contact with the foam mat. Stretching or bunching of the foam mat under the glass flat must be avoided.

#### 4. CONCLUSIONS

In phase shifting interferometers with horizontally mounted reference flat for precision metrology of planarity, the calibration of the reference flat remains a challenging problem because only the rotationally variant part of the deflection of the reference flat due to its weight can be determined as part of three-flat calibration procedures. A separate measurement of the deflection is required for the calibration of an interferometer with low uncertainty. We have demonstrated that the characteristic mechanical properties of polymer foam materials are useful for the isostatic, deflection-free support of optical precision flats. The foam support enables measuring the deflection of cylindrical reference flat due to gravity with an uncertainty at the nm level. We found that polyurethane foams have mechanical properties that make them well suited as isostatic support materials for optical precision flat and they appear to be available in a wide range of compressibilities. The main disadvantage of polyurethane foams is their visco-elastic behavior. In phase shifting interferometers that require stable cavities, settling times of several hours must be maintained after a flat is placed on the foam support, before the foam has sufficiently relaxed and measurements can be made.

#### Acknowledgments

We are indebted to Dr. Gale A. Holmes of the Material Measurement Laboratory at NIST for giving us access to a polymer testing machine and teaching one of us (U.G.) how to measure stress-strain diagrams. We are grateful to Bob F. Oreb, Australian Centre for Precision Optics, CSIRO, Australia, for helpful discussions of the early development of the calibration procedures for the LADI interferometer at CSIRO.

†**Disclaimer:** The full description of the procedures used in this paper requires the identification of certain commercial products and their suppliers. The inclusion of such information should in no way be construed as indicating that such products or suppliers are endorsed by either NIST or CSIRO, or are recommended by either NIST or CSIRO, or that they are necessarily the best materials or suppliers for the purposes described.

#### REFERENCES

- [1] Schulz, G. and Schwider, J., "Interferometric testing of smooth surfaces," *Prog. Opt.* **13**, 93–167 (1976).
- [2] Parks, R. E., "Removal of test optics errors," in [*Advances in Optical Metrology I*], Balasubramanian, N. and Wyant, J. C., eds., *Proc. SPIE* **153**, 56–63 (1978).

- [3] Fritz, B. S., "Absolute calibration of an optical flat" *Opt. Eng.* **23**, 379–383 (1984).
- [4] Evans, C. J. and Kestner, R. N., "Test optics error removal," *Appl. Opt.* **35**, 1015–1021 (1996).
- [5] Freischlad, K. R., "Absolute interferometric testing based on reconstruction of rotational shear," *Appl. Opt.* **40**, 1637–1648 (2001).
- [6] Küchel, M. F., "A new approach to solve the three fla problem," *Optik* **112**, 381–391 (2001).
- [7] Griesmann, U., "Three-fla test solutions based on simple mirror symmetry," *Appl. Opt.* **45**, 5856–5865 (2006).
- [8] Vannoni, M. and Molesini, G., "Iterative algorithm for three fla test," *Opt. Express* **15**, 6909–6816 (2007).
- [9] Griesmann, U., Wang, Q., and Soons, J. A., "Three-fla tests including mounting-induced deformations," *Opt. Eng.* **46**, 093601 (2007).
- [10] Burke, J. and Oreb, B. F., "The last word on three-fla calibration - are we there yet ?," in [*Fringe 2009, 6th International Workshop on Advanced Optical Metrology*], Osten, W. and Kujawinska, M., eds., 309–316, Springer (2009).
- [11] Vannoni, M. and Molesini, G., "Three-fla test with plates in horizontal posture," *Appl. Opt.* **47**, 2133–2145 (2008).
- [12] Dew, G. D., "The measurement of optical flatness" *J. Sci. Instrum.* **43**, 409–415 (1966).
- [13] Bünnagel, R., "Untersuchungen über die Eignung eines Flüssigkeitsspiegels als Ebenheitsnormal," *Zeitschrift für angewandte Physik* **8**, 342–350 (1956).
- [14] Debenham, M. and Dew, G. D., "Determining gravitational deformation of an optical fla by liquid surface interferometry," *Precis. Eng.* **2**, 93–97 (1980).
- [15] Powell, I. and Goulet, E., "Absolute figur measurements with a liquid-fla reference," *Appl. Opt.* **37**, 2579–2586 (1998).
- [16] Fairman, P. S., Ward, B. K., Oreb, B. F., Farrant, D. I., Gilliland, Y., Freund, C. H., Leistner, A. J., Seckold, J. A., and Walsh, C. J., "300-mm-aperture phase-shifting Fizeau interferometer," *Opt. Eng.* **38**, 1371–1380 (1999).
- [17] Oreb, B. F., Farrant, D. I., Walsh, C. J., Forbes, G., and Fairman, P. S., "Calibration of a 300-mm-aperture phase-shifting Fizeau interferometer," *Appl. Opt.* **39**, 5161–5171 (2000).
- [18] Gibson, L. J. and Ashby, M. F., [*Cellular solids*, 2<sup>nd</sup> ed.], Cambridge University Press (1997).
- [19] Lakes, R., [*Viscoelastic materials*], Cambridge University Press (2009).
- [20] Andersen, H. C., [*The princess and the pea (in Danish)*], C. A. Reitzel, Copenhagen (1835).
- [21] Love, A. H., [*A Treatise on the Mathematical Theory of Elasticity*, 4<sup>th</sup> edition], Dover Publications (1944).
- [22] Lur'e, I. A., [*Three-dimensional problems of the theory of elasticity*], Wiley & Sons (1964).
- [23] Selke, L. A., "Theoretical elastic deflection of a thick horizontal circular mirror on a ring support," *Appl. Opt.* **9**, 149–153 (1970).